Dissecting the toxicity and mitigating the impact of harmful Prymnesium blooms in the UK waters of the Norfolk Broads

Ben A. Wagstaff[1,2]*, Jennifer Pratscher[3,4]*, Peter Paolo L. Rivera[5], Edward S. Hems[1], Elliot Brooks[3], Martin Rejzek[1], Jonathan D. Todd[5], J. Colin Murrell[3], Robert A. Field[1,6]

*These authors contributed equally to this study
*Corresponding authors: ben.wagstaff@live.co.uk, jpratscher@gmx.de

[1] Department of Biological Chemistry, John Innes Centre, Norwich Research Park, Norwich, NR4 7UH, United Kingdom
[2] Present address: School of Life Sciences, University of Dundee, Dundee, DD1 5EH, United Kingdom
[3] School of Environmental Sciences, University of East Anglia, Norwich Research Park, Norwich, NR4 7TJ, United Kingdom
[4] Present address: Lyell Centre for Earth and Marine Science and Technology, Heriot-Watt University, Edinburgh, EH14 4AP, United Kingdom
[5] School of Biological Sciences, University of East Anglia, Norwich Research Park, Norwich, NR4 7TJ, United Kingdom
[6] Present address: Department of Chemistry and Manchester Institute of Biotechnology, University of Manchester, Manchester, M1 7DN, United Kingdom

Abstract

Prymnesium parvum is a toxin-producing microalga that causes harmful algal blooms (HABs) globally, frequently leading to massive fish kills that have adverse ecological and economic implications for natural waterways and aquaculture alike. The dramatic effects observed on fish are likely due to algae-produced polyether toxins, known as the prymnesins, but these compounds had not been detected in environmental samples, which has resulted in ambiguity about the true ichthyotoxic entities. Using qPCR, we found elevated levels of both *P. parvum* and its lytic virus, PpDNAV-BW1, in a fish-killing bloom on the Norfolk Broads, United Kingdom, in March 2015, a site historically plagued by *P. parvum* blooms. 16S rRNA gene sequencing confirmed that *P. parvum* dominated the bloom microbial community and that the microbial species diversity changed after recovery of the ecosystem. We also detected, for the first time, the recently discovered B-type prymnesin toxins in Broads waterway samples and gill tissue isolated from a dead fish taken from the study site. Furthermore, Norfolk Broads *P. parvum* isolates unambiguously produced B-type toxins in laboratory-grown cultures. In addition, a 2-year longitudinal study of the Broads study site showed *P. parvum* blooms positively correlated with increased temperature and that PpDNAV plays a significant role in *P. parvum* bloom demise in this natural setting. Finally, we used a field trial to show that treatment with low doses of hydrogen peroxide represents an effective strategy to mitigate blooms of *P. parvum* in enclosed water bodies.

Introduction

In a world with a rapidly growing human population, it has been estimated that since 1961 the average annual increase in consumption of fish (3.2 percent) has outpaced population

growth (1.6 percent), with further increased demand expected for the coming decade (1). This demand will be met by aquaculture, with an expected net decrease in wild fish consumption during this period (1). Harmful algal blooms (HABs) not only damage natural environments, but also represent a major threat to aquaculture; the rapid spread of algae can lead to fish stock losses through release of algal toxins, mechanical damage to gills, or water hypoxia associated with bloom collapse (2). One group of microalgae known for their bloom-forming ability are the haptophytes, made famous by the coccolithophore *Emiliania huxleyi*, which forms blooms tens of kilometres wide that can be seen readily by satellite imagery due to the reflective properties of its' coccoliths (3). On the other hand, the *Prymnesium* genus of the haptophytes has gained attention due to its' HABs that damage fish stocks globally, in both aquaculture and capture fishery industries (4).

Often referred to as 'golden algae', *P. parvum* has caused particular issues for aquaculture in North America in the last 2 decades. As a result, the biotic factors that impact *P. parvum* growth and toxicity have been studied extensively in laboratory settings (5-7). Although there has been speculation regarding the toxic entity responsible for fish deaths (8), it is now generally accepted that the ichthyotoxic (prymnesins) are the causative agents, due to their structural similarity to other ladder-frame polyether phycotoxins (9). However, the prymnesins have not previously been detected in a natural setting. First isolated by Igarashi and co-workers in 1995 (10-12), the prymnesins are a group of polyketide metabolites that display potent ichthyotoxicity (Figure 1). Since their discovery, a chemically diverse family of prymnesins, including prymnesin-B1, have been discovered (13-15), largely differing in the polyether core, glycosylation patterns, and level of chlorination of the toxins. More broadly, although research has identified certain environmental stimuli for bloom propagation [reviewed by Watson (16)], detailed insight into natural blooms and their seasonal cycles is lacking. Furthermore, whilst it has been shown that the use of algaecides or the addition of clay flocculants or barley straw, can effectively kill or inhibit the growth of *P. parvum* (17-19), this research has yet to translate into effective strategies for combatting HABs.

Figure 1 | Chemical structure of prymnesin-1, -2, and -B1. (10, 13). Adapted from Hems *et al.* (14).

Detailed studies of HABs in the natural environment are limited and warrant investigation. Here, we investigated the effects of a *P. parvum* HAB on Hickling Broad, England, an area frequently plagued by blooms of this organism, but where the responsible ichthyotoxins were not previously known (20, 21). The Norfolk Broads are a shallow, man-made set of navigable brackish lakes arising from flooded peat extraction that dates back to the 12th century. These waterways are a haven for birds and other wildlife, and a tourist attraction that is used for boating and angling throughout the year. The Broads are thought to contribute approximately £550 million per year to the local economy (22), which is threatened by frequent blooms of cyanobacteria and *P. parvum*. Hickling Broad, in particular, has had recurrent blooms of *P. parvum* since they were first reported in the 1960's, but incidents are thought to date back to at least the early part of the 20th century (20).

Using molecular genetic approaches, we show that *P. parvum* dominated the microbial community during the toxic bloom on Hickling Broad in 2015. We also show how the microbial community composition changes under non-bloom conditions. Using biochemical methods,

we report for the first time the detection of trace levels of prymnesin toxins in natural water samples and gill cells of a dead fish recovered during the *P. parvum* bloom of 2015. We support these findings by isolation of the local strain of *P. parvum* found on Hickling Broad and the use of targeted metabolomics to conclusively show production of the B-type prymnesins in these strains. Furthermore, we followed population dynamics of *P. parvum* and its' lytic virus, PpDNAV-BW1 (23) over a 2-year period. We conclude by showing that hydrogen peroxide provides an effective mitigation strategy for *Prymnesium* bloom incidents. This multi-disciplinary study sheds light on natural bloom dynamics of an important fish pathogen and provides the basis for understanding and managing future *Prymnesium* blooms in enclosed water bodies.

Materials and Methods

Study site, water sampling, and processing

Hickling Broad was chosen as a study site due to repeated instances of *P. parvum* blooms (20) and an active bloom incident in April 2015 that we were able to monitor. Eleven sampling locations were initially chosen to cover a large area of the broad, which was later expanded to include sampling point 12 that is not included in some analyses (Figure 2). In addition to the bloom samples from April 2015, full sets of water samples from all sampling points on Hickling Broad were taken every 2-4 weeks from January 2016 until December 2017. For every sampling point, two sterile 50 ml Falcon tubes were filled with water (100 ml total per sample) from ~ 20 cm depth, making sure to exclude the surface layer. Biomass in Falcon tubes was pelleted by centrifugation at 3,200 x *g* and 4°C for 10 min. Duplicate pellets were resuspended in 1 ml of nuclease free water (Ambion, Thermo Fisher Scientific) and suspensions from the same sampling point were pooled. Cell suspensions were subsequently pelleted at 18,000 x *g* at 4°C for 10 min, supernatant was discarded, and cell pellets were flash frozen with liquid nitrogen and stored at -80°C until further processing. In addition, for every sample, pH, temperature and conductivity measurements were recorded. Sampling maps were generated using the QGIS 2.18 package (http://qgis.osgeo.org) with the OSM standard map.

Figure 2 | Map of wider Norfolk and sampling points on Hickling Broad. Top – Map of Norfolk and the Hickling Broad highlighted by a red circle. Bottom - Map showing the sampling points covering Hickling Broad established during the harmful *P. parvum* bloom in April 2015 and retained throughout the whole sampling campaign. The red shaded area represents the area where the majority of fish kills were observed during the bloom. Sample point 12 was added later as an additional sampling point and is not included in some analyses. Map was generated using QGIS with OSM standard map. Scale bar (top) – 30 km. Scale bar (bottom) – 1 km.

Nucleic acid extraction from water samples

Nucleic acids were extracted from water and sediment using a sodium dodecyl sulfate (SDS)-based protocol (24) with minor modifications. The biomass pellet of 100 ml Hickling Broad water were added to a 2.0 ml screw-cap tube of Lysing matrix E beads (MP Biomedicals UK) and mixed with 1 ml of 2.5% SDS extraction buffer. Cells were lysed in a FastPrep instrument (MP Biomedicals UK) for 45 s at 6.0 m s^{-1} and supernatants were extracted twice using phenol:chloroform:isoamyl alcohol (25:24:1) and chloroform:isoamyl alcohol (24:1). Nucleic

acids were precipitated with polyethylene glycol (PEG) 6000 solution (20 %) and dissolved in 100 µl of nuclease free water (Ambion, Thermo Fisher Scientific). Bloom (April 2015) and non-bloom (September 2016) RNA samples were further reverse transcribed with random hexamer primers (Invitrogen) and M-MLV reverse transcriptase (Promega) for 16S rRNA amplicon sequencing.

16S rRNA gene amplicon sequencing for water and sediment samples

The pooled biological replicates for DNA and cDNA samples from Hickling Broad water from bloom (April 2015) and non-bloom (September 2016) samples, as well as the DNA samples from the hydrogen peroxide trial (June 2017) were selected for 16S rRNA/rDNA amplicon sequencing. The primer set 515F/806R of the V4 variable region of the 16S rRNA gene (25) was used for amplification. Amplification and amplicon sequencing were performed by MR DNA (Shallowater, TX, USA). Sequencing was performed on a MiSeq system according to manufacturer instructions, obtaining between 106k-257k reads per sample with an average length of 300 bp. Resulting datasets were analysed by sequence analysis and phylogenetic classification using QIIME 1 (26).

Specific qPCR for *P. parvum* and PpDNAV

The abundance of *P. parvum* internal transcribed spacer (ITS) copies in the water was quantified by qPCR using primers PrymF (27) and PrymR-3 (28) as previously described (28). The 25 µL reaction mixture contained 12.5 µL of SYBR® Green JumpStart™ Taq ReadyMix™ (Merck), 0.15 µM of each primer, 200 ng BSA ml^{-1}, 3.0 mM $MgCl_2$, and 2.0 µL template DNA.

For the *P parvum* virus PpDNAV, qPCR primers were designed to the major capsid protein 1 (*mcp1*) gene of the PpDNAV. Isolate (23) using the ARB software package (29) based on the genome sequences recovered from the PpDNAV isolate (23). The resulting specific primer pair was named MCP1-1F (CCGTAATCCAGGTCTCGCTC) and MCP1-1R (CAAGGGAACTGACAGCCCAT) and amplified a 110 bp long fragment. The PpDNAV *mcp1* qPCR temperature profile consisted of an initial denaturation at 95 °C for 3 min and 35 cycles of denaturation, annealing and extension at 95, 69.8 and 72 °C for 30, 40 and 40 s, respectively, followed by a melting curve from 60-95 °C in 0.3 °C increments. The 25 µL reaction mixture contained 12.5 µL of SYBR® Green JumpStart™ Taq ReadyMix™ (Merck), 0.3 µM of each primer, 200 ng BSA ml^{-1}, 3.0 mM $MgCl_2$, and 1.0 µL template DNA. The efficiency for this qPCR assay was 98%. All assays were performed in a StepOnePlusTM Real-Time PCR System (Applied Biosystems) in triplicates, respective qPCR standards were used, and controls were run with water instead of DNA or cDNA extract.

Isolation of *P. parvum* Hickling strains

P. parvum strain HIK PR1A (clone 1A) and HIK PR6H (clone 6H) were isolated from Hickling Broad, Norfolk, UK (52°44’48.3”N, 1°34’10.8”E) during a minor bloom of *P. parvum* in June 2017. In brief, water from Hickling broad (50 ml) was inoculated into F/2 medium - Si (100 ml, 5 PSU) (30). Several strains of *P. parvum* were isolated and made monoclonal by micropipetting single cells through rinses of sterile medium (31) and plated into 96 -well plates. Isolates were allowed to grow for 2-3 weeks at a constant temperature of 22°C under

a 12:12h light:dark photoperiod with a constant photon flux of 120 µE m^{-2} s^{-1} (QSL-100 Quantum Scalar Irradiance Meter, Biospherical Instruments, San Diego, USA) provided by Philips MASTER TL-D 58W/840 white tubes. Isolates from enriched cultures were further enriched by removing contaminating picoplankton by dilution. Enriched strains were transferred to 42-well plates and allowed to grow for approximately 2-3 weeks. Cultures were then made axenic by treatment with multiple rounds of antibiotics (400 µg ml^{-1} of streptomycin, 50 µg ml^{-1} of chloramphenicol, 20 µg ml^{-1} of gentamicin and 100 µg ml^{-1} of ampicillin). The absence of contaminating bacteria was confirmed by epifluorescence microscopy of culture samples stained with DAPI (32). Clonal cultures were then carefully transferred and up-scaled to 75 cm^2 cell culture flasks (Nunc™ EasyFLASK with Filter Caps, ThermoFisher Scientific) containing 20-40 ml modified F/2 medium -Si. The growth of monoclonal strains was monitored every 3 days using a CASY cell counter (Innovatis, Reutlingen, Germany) to confirm that the cells were growing normally (Supplementary Figure 1).

Toxin detection using LC-MS

For the extraction and LC-MS-based analysis of prymnesins from cultured *P. parvum* HIK PR1A and HIK PR6H, the procedure outlined in Hems *et al.* was followed (14). For the extraction of prymnesins from natural water samples, 100 ml of water taken from Location 6 and 7 (Figure 2) was centrifuged at 3000 x *g* to pellet cells and debris. The resulting supernatant was then filtered using a 0.45 µm filter and next passed through a 1 g C18 cartridge (Sep Pak) at a flow rate of 1 ml^{-1} to load prymnesins. The cartridge containing the water-extracted prymnesins was then washed with 5 column volumes of water, before elution of toxins with 10 column volumes of 80% *n*-propanol in water. For the extraction of prymnesins from fish gill plates, the latter were first excised from the fish using a scalpel, before grinding of the cells under liquid nitrogen using a pestle and mortar. At this point, the mascerated material was extracted with cold acetone and prymnesins were isolated according to the protocol for *P. parvum* cells as described by Hems *et al.* (14). The resulting dried samples after methanol and *n*-propanol extraction were resuspended in water and loaded onto, and eluted from, a 1 g C18 cartridge in the same manner as described above for the water extracted prymnesins.

The column eluates were then dried under vacuum using a rotary evaporator and resuspended in 2 ml water. The samples were next 'defatted' by adding EtOAc to a 1:1 ratio, shaken vigorously to ensure sufficient mixing of the phases, then allowed to sit and the aqueous and organic layers separated. The EtOAc layers were removed. This process was repeated a further 3 times, before the remaining aqueous fractions were again dried and re-suspended in 200 µl 0.1% TFA and subject to LC-MS analysis.

Hydrogen peroxide trial

A narrow dyke close to location 6 (Whispering Reeds Boatyard back lagoon, approx. volume 730 m^3) was chosen as the field trial site for hydrogen peroxide application as it was easily accessible from the bank side and it was the site where thousands of fish congregated during the toxic bloom in April 2015. The target concentration of hydrogen peroxide (40-50 mg/L) was achieved by application of hydrogen peroxide stock (35 w/w %) using 2 bank fixed jets (Oxyjet 50). To ensure efficient mixing a water aerator unit, set up in the centre of the dyke,

was employed. Concentration of hydrogen peroxide was monitored using Quantofix test strips (Peroxide 100, Sigma Aldrich, UK). The target concentration was maintained for up to 3 hours after application. 5 sampling locations were chosen; 3 within the dyke directly adjacent to the area being treated with H_2O_2, and 2 negative controls outside of the dyke (see Fig. 8a). Water samples were collected from all sampling points before (T0) and 1, 4, 6, 24, 96, and 456 hours after hydrogen peroxide application. The water samples were used for nucleic acid extraction and for qPCR and 16S rRNA gene amplicon sequencing as described above. For each sample, pH, temperature and conductivity measurements were taken.

Results

Study site – Hickling Broad

A toxic bloom of *P. parvum* on Hickling Broad, Norfolk, England was first reported by members of the public on 13th March 2015 when multiple fish mortalities were observed. Subsequently, the site was visited on 17th March 2015 and water samples were taken from 12 locations across the broad for further analysis (Figure 2).

Quantification of *P. parvum* and PpDNAV in water samples from a toxic bloom

Total DNA extracted from water samples taken during the toxic bloom of 2015 was analysed by qPCR for the marker genes of both *P. parvum* and its' lytic virus, PpDNAV (23). A technical triplicate of results suggested a severe bloom of *P. parvum* was ongoing, with copy numbers of the internal transcribed spacer (ITS) region of *P. parvum* DNA reaching almost 12 x 10^6 copies ml^{-1} of water at location 6. This represented an on average 1,000-1,500 times higher number than seen in non-bloom conditions, as discussed later. In general, *P. parvum* was seen in higher abundance at sampling locations towards the most northerly point of the Broad (Figure 3), particularly location 6, which fell within a very shallow, sandy dyke near to a waterside restaurant and pleasure craft boatyard. Location 7 was an exception to this trend, but the sighting of severe cases of what appeared to be fungi (Supplementary Figure 2) near this location were noted as a potential reason for the lack of *P. parvum* observed at this location.

We recently showed that *P. parvum* can be infected by a lytic virus, PpDNAV (23), which was isolated from this location. Thus, we next sought to determine whether the bloom of *P. parvum* in 2015 was infected by PpDNAV. Using the same DNA samples obtained from the water samples taken during the bloom, we performed qPCR with primers designed to specifically amplify the major capsid protein (*mcp1*) gene of PpDNAV. Results from these qPCR experiments showed 12-1,000 times higher copy numbers of *mcp1* at location 6 compared to the other sampling locations, suggesting active infection was occurring at this location during our sampling regime (Figure 3). Levels of *mcp1* at other sampling locations remained lower or in some cases undetectable, suggesting that populations of *P. parvum* at these locations were not infected by PpDNAV. It is interesting to note that levels of algal ITS reads did not correlate directly with fish deaths, which required both high levels of algal ITS reads and viral *mcp1* reads. For example, sampling locations 10 and 11 showed higher algal ITS reads than most other sampling locations but very few PpDNAV *mcp1* reads and few/no observable fish deaths nearby. Conversely, location 6 showed high algal ITS reads and high PpDNAV1 *mcp1* reads

with many observable fish mortalities and distressed fish (Supplementary Figure 3). It is therefore tempting to speculate that viral presence, or *P. parvum* bloom demise as a result of viral infection, is required for bloom ichthytoxicity: this idea warrants further study.

Figure 3 | Abundance of *P. parvum* and PpDNAV in Hickling Broad water samples during the harmful bloom in April 2015. Abundance of *P. parvum specific* ITS genes (light grey bars) and PpDNAV *mcp1* genes (dark grey bars) was measured by qPCR of total DNA extracted from Hickling Broad water samples collected during the harmful *P. parvum* bloom in April 2015. Values represent the average of three replicates with their respective standard deviations. Numbers refer to sampling sites on Hickling Broad (see Fig. 1).

Community composition during a bloom compared to non-bloom conditions

To investigate the effect of the *P. parvum* bloom on the microbial ecosystem, we performed 16S rRNA gene microbial community analysis during the bloom and during non-bloom conditions (Figure 4). Results during the bloom showed that *P. parvum* chloroplast 16S rRNA genes dominated the ecosystem in all sampling locations examined, representing between 20% and 41% of the total microbial community in location 9. During non-bloom conditions, levels of *P. parvum* were as low as only 2% of the total population, and a much more diverse microbial community was seen.

Interestingly, the bloom of *P. parvum* coincided with elevated levels of *Rhodobacterales*, specifically *Marivita* (up to 25% abundance) compared to non-bloom conditions (5%). This was also observed for *Saprospirales*, specifically *Lewinella* (up to 20% bloom vs 4% non-bloom) and *Rhodocyclales*, specifically *Methyloversatilis* (up to 5% bloom vs 0.8%). Some of these microorganisms have been described as versatile methylotrophs (*Methyloversatilis*) or complex carbohydrate degraders (*Lewinella*), so might benefit from the increased cell biomass being made available during the bloom (33, 34). *Marivita* species have further been shown to co-occur with a wide range of algae and have therefore been postulated to be growth-promoting algal symbionts (35). Conversely, during non-bloom conditions cyanobacterial genera such as *Microcystis* (up to 0.03% bloom vs 12.4% non-bloom), *Cytophaga* (up to 0.05% bloom vs 7.5% non-bloom), and *Synechococcus* (up to 2% bloom vs 16.5% non-bloom) were more abundant, in an overall more diverse microbial community. The same community pattern observed in the DNA samples could be observed in the cDNA 16S rRNA profiles (Supplementary Figure 4) indicating no significant differences between present and active microorganisms in the water samples during bloom and non-bloom.

Figure 4 | Microbial community profiles of the harmful *P. parvum* bloom compared to non-bloom water on Hickling Broad, obtained by 16S rRNA gene amplicon sequencing. Profiles are derived from total DNA extracted from Hickling Broad water samples collected at consistent sampling points during the harmful *P. parvum* bloom in April 2015 and during a non-bloom phase in September 2016. Relative abundance of taxonomic groups within each sample is shown at the order level as percentages. Only taxa with a combined relative abundance of $\geq$ 0.1% are shown. Numbers refer to sampling sites on Hickling Broad (see Fig. 1).

Detection of prymnesins in environmental water samples and fish gill cells

We next sought to detect the prymnesin toxins from environmental water samples. Although they are implicated in fish mortality worldwide and have previously been extracted and detected from laboratory-grown cultures of *P. parvum*, the prymnesins have yet to be detected from environmental water samples nor from their speculated targets (gill cells of fish). We therefore applied a modified version of the extraction method of Manning *et al* (36). For extraction of prymnesins from water, samples taken from location 6 and 7 during the toxic bloom of 2015 were passed through a solid-phase C18 cartridge and prymnesins were eluted with 2 separate elutions of *n*-propanol and methanol. For the extraction of prymnesins from gill plates, a dead pike (*Exos lucius*) was recovered from the toxic bloom and the gill plates were excised from the fish, macerated with a pestle and mortar and extracted using a combination of solvent extraction and solid-phase extraction, according to Manning *et al* (36). Both samples were then analysed using LC-MS, as previously described (14). No signals corresponding to prymnesin-1 or prymnesin-2 were detected for either water or gill-extracted samples. Upon further examination, masses corresponding to the aglycone backbone of prymnesin-B1, recently discovered by Rasmussen *et al*., (13) could be tentatively detected (Figure 5). Extracted-ion chromatograms suggested the B-type prymnesins were present in gills of a dead pike and from a water sample taken at location 6 (Figure 5A). High background prevented the detection of these compounds from a water sample taken at location 7. This agrees with the findings of higher levels of *P. parvum* at location 6 during the bloom, as reported above.

Figure 5 | MS-based identification of B-type prymnesins from environmental samples and isolates of *P. parvum* from Hickling Broad. (**A**) ESI-MS spectrum showing detection of the diagnostic signal (m/z 828.8963, Δ -0.6 ppm) for the backbone of the B-type prymnesins from Pike gill cells (top), and water sample 6 (bottom) taken during a toxic bloom. ESI-MS signal corresponding to the singly glycosylated form of the toxin (m/z 909.9246, Δ 1.54 ppm) could also be seen in the water sample from location 6. (**B**) Light microscopy images of *P. parvum* HIK PR1A (left) and HIK PR6H (right). (**C**) ESI-MS spectra showing detection of the diagnostic signals for the aglycone (m/z ~828.9), mono glycosylated with a pentose (m/z ~894.9), mono glycosylated with a hexose (m/z ~909.9), and double glycosylated with pentose and hexose (m/z ~ 975.9) forms of the B-type prymnesins, from HIK PR1A (left) and HIK PR6H (right). All masses observed for the toxins have errors less than Δ 3 ppm with the exception of m/z 975.9407 of the intact double glycosylated toxin from HIKPPR-6H which has an error of Δ -3.8 ppm. (**D**) Schematic of proposed prymnesin-B fragmentation events observed in ESI-MS spectra (A) and (C). Losses of m/z = 66 or m/z = 81 correspond to the loss of pentose or hexose units from the toxin backbone, respectively.

Detection of prymnesins from strains of *P. parvum* isolated from the study site

Due to low sample availability and the evidently low concentration of suspected toxins present in natural samples, we next sought to isolate a strain of *P. parvum* from Hickling Broad and extract toxins from dense cultures of laboratory grown algae to unambiguously confirm their identity. *P. parvum* was isolated and made axenic by a combination of single-cell micropipetting and antibiotic treatments (31), which resulted in two strains of *P. parvum*, HIK PR1A and HIK PR6H (Figure 5B), which were then both examined for their production of

prymnesin toxins. Cultures of both strains were grown to late logarithmic phase, harvested, and their prymnesins extracted as previously described (14). Both strains gave similar toxin profiles, and were confirmed to produce the B-type prymnesins, as expected (Figure 5C). In addition to detecting signals corresponding to prymnesin-B1 that contains 1 hexose sugar, we were also able to detect m/z signals corresponding to the same toxin backbone but glycosylated with a pentose sugar (prymnesin-B2 (13)), and the toxin with both a hexose and pentose which Rasmussen *et al.* detected in *P. parvum* strains from Denmark, Norway and Australia (13) (Figure 5B). Due to a low separation of these species under our chromatography conditions (Supplementary Figure 5), it is unclear whether the organism produces a mixture of these forms of the toxin (Figure 5D), or whether the loss of m/z values corresponding to these sugars is an artefact of mass spectrometry fragmentation, as is frequently the case for this class of compounds (13, 14, 36).

Seasonal dynamics of *P. parvum* and PpDNAV over a 2-year period

Using qPCR we next sought to follow seasonal populations of *P. parvum* on Hickling Broad and to determine whether blooms are regulated/controlled by viral infections of *P. parvum* with PpDNAV. Water samples were taken bi-monthly over a 2-year period and total DNA was extracted and subjected to qPCR using the previously described *P. parvum* (ITS) and PpDNAV (*mcp1*) primers. These data showed that the abundance of *P. parvum* and PpDNAV positively correlated with air/water temperature, which is known to affect the frequency and severity of *Prymnesium* blooms (7, 37) (Figure 6). For levels of *P. parvum*, the sampling sites displayed a similar seasonal trend, but location 6 consistently showed higher *P. parvum* numbers than the average for the whole Broad, agreeing with previous data for the toxic bloom of 2015. Furthermore, the two-year time course showed that blooms of *P. parvum* strongly correlate with an increase in temperature, where the major 2 blooms of the study both occurred in the warmer months of August 2016 and June 2017 when the temperature was higher (21 ^{o}C for August 2016 and 27 ^{o}C for June 2017). Smaller blooms of *P. parvum* were observed throughout the later summer months and leading into Autumn (August to October) but levels of *P. parvum* remained low consistently throughout Winter and Spring (November to May) where temperatures were at their lowest.

Copy numbers for PpDNAV *mcp1* displayed a similar trend, but appeared to reach highest values shortly after those for *P. parvum* values reached their highs, during a crash of the algal populations. The first bloom of *P. parvum* reached its' peak on 18th August 2016 which was followed by a peak of PpDNAV 3 weeks after on 6th September 2016. A subsequent smaller bloom of *P. parvum* was observed at location 6 on 18th October 2016 and this was again followed by a sharp rise in PpDNAV levels shortly after on 1st November 2016. This pattern was also seen for the major bloom of *P. parvum* in 2017 on 6th June where viral transcripts saw a sharp peak on the same date, and also shortly after the algal bloom on 3rd July 2017. Interestingly, viral numbers saw a small, prolonged rise throughout the early months of 2017 (January to April) whilst values for *P. parvum* during this time remained very low. The opposite was also observed in 2017 after the major bloom of *P. parvum* had occurred; smaller blooms of *P. parvum* were noted with no observed rise in viral numbers during this period.

Figure 6| 2-year survey of *P. parvum* and PpDNAV population dynamics on Hickling Broad. Abundance of *P. parvum* specific ITS genes and PpDNAV *mcp1* genes was measured by qPCR

of total DNA extracted from Hickling Broad water samples collected at consistent sampling points every 2-4 weeks from January 2016-January 2018 (see Fig. 2). Values represent the average of three replicates with their respective standard deviations.

Mitigation of *P. parvum* blooms with hydrogen peroxide and its impact on microbial community composition

The Norfolk Broads are a National Park and as such the use of chemical algaecides are not permitted. However, the Environment Agency that have responsibility for managing the Broads already use dilute hydrogen peroxide for the aeration of hypoxic water; a chemical that, at higher concentrations, has previously been shown to reduce levels of cyanobacteria (38), toxic phytoplankton (39) and even their corresponding toxic metabolites (39). We therefore set about determining whether low doses of hydrogen peroxide could be an effective treatment method for blooms of *P. parvum*. Preliminary laboratory studies identified that a concentration of 40 mg/L of H_2O_2 was sufficient to reduce late-logarithmic phase (~3,000,000 cells ml^{-1}) *P. parvum* populations by >97 % over a 72-hour time period (Supplementary Figure 6). Following approval from the Norfolk Wildlife Trust, hydrogen peroxide dosing trials were carried out close to location 6 (Figure 2), in a small dyke where fish were seen to congregate during the toxic bloom of 2015 (Figure 7A). Hydrogen peroxide was applied and concentrations were raised to the target 40-50 mg/L (Figure 7A – red square). Water samples were taken regularly at 3 locations close to the site of H_2O_2 application (locations 1, 2 ,3), and 2 further sites outside of the dyke that would act as negative controls (locations 6 and 7). Water samples taken from these locations were extracted for cellular DNA and a combination of qPCR analysis (Figure 7B) and 16S community profiling (Figure 7C) was carried out to assess the impact of H_2O_2 dosing on *P. parvum* levels and the overall balance of the microbial community. qPCR analysis using primers designed to amplify the ITS region of *P. parvum* showed that before treatment levels of *P. parvum* were considerably lower than in bloom conditions (200-500 copies ml^{-1} vs highs of 12,000,000 copies ml^{-1}). Levels of *P. parvum* started to fall as little as 2 hours after dosing with hydrogen peroxide (Figure 7B). These low levels remained low in locations 1, 2, and 3 relative to the control locations (6 and 7) over the subsequent 24 hours. Levels of *P. parvum* at the treatment site were seen to recover to normal levels relative to the control locations 96 hours after H_2O_2 treatment, suggesting no adverse prolonged effects on the local *P. parvum* population in this open water system.

16S rRNA gene amplicon sequencing was carried out to look at the overall effect of hydrogen peroxide treatment on the microbial community (Figure 7C). Before treatment, little differences in relative percentage abundance of taxonomic groups between sampling locations was observed. However, 1 hour after H_2O_2 treatment noticeable changes could be observed in relative abundances of taxonomic groups between treated locations (1, 2, and 3) versus control locations (6 and 7). The largest noticeable effect was on the relative abundance of *Chroococcales* (largest green bars) which dropped from 24% abundance in location 3 to 5% relative abundance just 1 hour after peroxide treatment. *Chroococcales*, such as the genera *Microcystis* and *Snowella*, are cyanobacteria and known to be susceptible to peroxide treatment (40).

Figure 7 | Effect of peroxide treatment on the abundance of *P. parvum* and microbial community profiles in Hickling Broad water samples. (**A**) Study site on Hickling Broad where hydrogen peroxide was applied (locations 1-3), and control locations outside of the dyke (locations 6, 7). Scale bar represents 100 m. (**B**) Abundance of *P. parvum specific* ITS gene was measured by qPCR of total DNA extracted from Hickling Broad water samples collected over a time series before (T0) and after *in situ* peroxide treatment (1 h, 4 h, 6 h, 24 h, and 96 h) in June 2017. Values represent the average of three replicates with their respective standard deviations. (**C**) Microbial community profiles derived from total DNA extracted from Hickling Broad water samples collected over a time series before (T0) and after *in situ* peroxide treatment (1 h, 4 h, and 6 h) in June 2017. Relative abundance of taxonomic groups within each sample is shown at the order level as percentages. Only taxa with a combined relative abundance of > 0.1% are shown. Numbers refer to sampling sites during the peroxide trial.

Discussion

P. parvum has plagued the Norfolk Broads with toxic blooms for over a century, damaging the ecosystem and the local economy of the otherwise thriving National Park (20). In this study, we took a multi-disciplinary approach to learn more about bloom dynamics of this harmful alga and its' lytic virus, PpDNAV, and provide potential solutions and future management strategies for blooms of this organism.

A toxic bloom of *P. parvum* on Hickling Broad was first reported on 13th March 2015 and ultimately resulted in thousands of fish deaths, with an estimated 600,000 fish manually relocated to safer waters over the course of the toxic episode. Inspection of the extent of the bloom and water sampling was subsequently carried out on 17th March 2015 where it was noted that the epicentre of the bloom was close to Location 6 at the most northerly point of the Broad (Figure 2 and Supplementary Figure 3). Initial qPCR experiments used to quantify the extent of the *P. parvum* bloom showed elevated transcript levels of *P. parvum* ITS gene and PpDNAV *mcp1* across the broad, but particularly in location 6 where numbers for *P. parvum* ITS surpassed 11,000,000 copies ml^{-1} water (Figure 3), agreeing with the observations of increase fish mortalities at Location 6. 16S rRNA gene profiling showed *P. parvum* dominated the microbial community during the bloom, with up to 41% of 16S reads assigned to *P. parvum* chloroplast 16S (Figure 4). This agrees well with the general idea that algae can establish dominant niches in communities under the right conditions (41). In a control timepoint under non-bloom conditions, *P. parvum* only made up 2% of the population, which also shows a higher diversity of abundant taxonomic groups. Cyanobacterial groups, such as *Microcystis*, *Cytophaga* and *Synechococcus*, in particular, seem to be supressed or outcompeted during blooms of *P. parvum* compared to non-bloom conditions (42).

Even though many metabolites produced by *P. parvum* have been implicated in fish mortality (43, 44), it is generally believed the toxic entities responsible for mass fish kills are the polyether prymnesins due to their potent ichthyotoxicity (8, 11). Although these toxins have been well described and detected in laboratory settings, before this study they had never been detected in environmental samples, leading to speculation about whether or not they are ecologically relevant to fish deaths. Using LC-MS methods, we first confirmed the presence of the recently discovered prymnesin-B1 (13) from a water sample taken from

location 6 and gill cells of a deceased pike taken during the Hickling Broad toxic bloom of 2015 (Figure 5A). To unambiguously confirm the toxin identity, we isolated *P. parvum* from the study site. Using single cell micropipetting, we were able to isolate two strains, HIKPPR-1A and HIKPPR-6H (Figure 5B) and show, using previously described methods (14), to show that both strains produce B-type prymnesins (Figure 5C). Interestingly, both strains appear to produce a doubly glycosylated form of the B-type prymnesins(13) (Figure 5D). Taken together, the combined detection of these toxins in environmental samples, as well as the confirmation that these same toxins are produced in a laboratory setting by *P. parvum* HIKPPR-1A and HIKPPR-6H isolated from the study site, strongly implies that the prymnesins are indeed the toxic entities responsible for mass fish mortalities during *P. parvum* blooms.

Using the established qPCR methodology, we next went on to follow levels of *P. parvum* and its' lytic virus, PpDNAV over a 2-year timeframe (Figure 6). Unlike the toxic bloom which occurred in April 2015 and previous findings of others that suggest blooms of *P. parvum* have no seasonality (20), we observed over these 2 years that blooms strongly correlated with increases in temperature. Large blooms of *P. parvum* were observed in summer months when temperature was at its highest and leading into autumn (August 2016 and June 2017), with smaller blooms occurring into Autumn. During the winter months, when temperatures were low, levels of *P. parvum* remained consistently low. Spikes in intracellular PpDNAV levels appeared to occur directly after blooms of *P. parvum* until the bloom declined, which suggests that PpDNAV is likely responsible for the demise of blooms of *P. parvum* in this natural environment, according to Lotka-Volterra predator:prey population dynamics (45). Interestingly, higher levels of both *P. parvum* and PpDNAV were consistently observed at sampling location 6 compared to other locations, as was seen for the toxic bloom of April 2015, suggesting other factors not considered in this study such as nutrient content or water movement may be contributing to the severity of blooms in this location.

Finally, we sought to develop a practical management strategy for the repeated occurrence of *P. parvum* blooms on Hickling Broad. Algaecides, barley straw, and flocculating clay have previously been shown to be effective in a laboratory setting (17-19), but have yet to translate to field use possibly due to their high costs or limits of the practical application of these strategies. Conversely, the use of low doses of hydrogen peroxide has previously been shown to be effective at treating large blooms of other toxic algae in natural environments, as well as reducing levels of the toxic metabolites they produce (38, 39). We first showed in a laboratory setting that low concentrations (40 mg/L) of H_2O_2 are effective at killing dense *P. parvum* cultures. These concentrations of H_2O_2 have previously been shown to cause little to no damage to selected fish species (46, 47). We next carried out field trials in a small dyke at the most northerly point of Hickling Broad (Figure 7A), where H_2O_2 was applied and water samples were taken at regular intervals to look for the effect of the treatment on *P. parvum* levels and the microbial community composition. We were able to use qPCR to show that levels of *P. parvum* were effectively reduced over the duration of the treatment and recovered to 'normal' levels relative to control levels 96 hours after treatment (Figure 7B). Furthermore, we showed that the application of H_2O_2 did not dramatically change the overall microbial community, although relative levels of *Chlorococcales* were particularly reduced by the treatment (Figure 7C). No adverse effects were noted over the course of the treatment for any macroinvertebrates or aquatic life. Coupled with the low cost of use, these results

suggest that low doses of H_2O_2 may constitute an effective treatment strategy for blooms of *P. parvum* on Hickling Broad.

In summary, in this study we report a toxic bloom of *P. parvum* in April 2015 that occurred on Hickling Broad in the UK and that resulted in many thousands of fish deaths. We show that *P. parvum* dominated the microbial community during this period and may have had a particularly negative effect on cyanobacterial species that were significantly more abundant under non-bloom conditions. We then undertook a 2-year sampling regime to follow seasonal bloom dynamics of both *P. parvum* and its' lytic virus, and were able to show that blooms of *P. parvum* positively correlated with an increase in temperature in this period, and that PpDNAV is likely a major contributor to bloom demise. Furthermore, we report the detection of prymnesins in natural water samples and the gill cells of a bloom-associated dead fish for the first time, supporting the argument that these toxins are the responsible entities for the mass fish mortalities observed during *P. parvum* blooms. Finally, we show that low doses of hydrogen peroxide are likely an effective and cheap treatment strategy for blooms of *P. parvum*, without adverse side effects on the microbial community or higher macroinvertebrates and aquatic life.

Acknowledgements

We thank Gerhard Saalbach for assistance with mass spectrometry. We would also like to thank John Currie, Steven Lane, Andrew Hindes, Gavin Devaney, and other colleagues from the Norfolk and District Pike Club, Environment Agency, Fishtrack Ltd and Norfolk Broads Authority, respectively, for invaluable insight and support.

Availability of data and materials

Amplicon sequence data generated in this study were deposited to the NCBI Sequence Read Archive (SRA) under BioProject ID PRJNA595342.

Funding

Work at the John Innes Centre is supported by the UK BBSRC Institute Strategic Program on Molecules from Nature - Products and Pathways [BBS/E/J/000PR9790] and the John Innes Foundation. B.A.W was supported by a BBSRC CASE PhD studentship with the Environment Agency. J.P was supported by a NERC Independent Research Fellowship (NE/L010771/2) and Norwich Research Park Science Links Seed Fund (SLSF 32). E.S.H was supported by a Norwich Research Park DTP PhD Studentship. P.R was supported by the Newton Fund Scholarship (261863799), a joint programme by the British Council and the Commission on Higher Education (CHED), Philippines. Work in the J.D.T laboratory was supported by the Natural Environmental Research Council standard grants NE/S001352/1 and NE/P012671/1. J.C.M research is also supported by the Earth and Life Systems Alliance, Norwich Research Park.

References

1. FAO. The State of World Fisheries and Aquaculture 2018 - Meeting the sustainable development goals. FAO Rome, Italy; 2018.
2. Smayda TJ. What is a bloom? A commentary. Limnol Oceanogr. 1997;42:1132-6.
3. Merico A, Tyrrell T, Brown CW, Groom SB, Miller PI. Analysis of satellite imagery for *Emiliania huxleyi* blooms in the Bering Sea before 1997. Geophys Res Lett. 2003;30:70-1.
4. Roelke DL, Barkoh A, Brooks BW, Grover JP, Hambright KD, LaClaire JW, et al. A chronicle of a killer alga in the west: ecology, assessment, and management of *Prymnesium parvum* blooms. Hydrobiologia. 2016;764:29-50.
5. Granéli E, Edvardsen B, Roelke DL, Hagström JA. The ecophysiology and bloom dynamics of *Prymnesium* spp. Harmful Algae. 2012;14:260-70.
6. Larsen A, Edvardsen B. Relative ploidy levels in *Prymnesium parvum* and *P. patelliferum* (Haptophyta) analyzed by flow cytometry. Phycologia. 1998;37:412-24.
7. Larsen A, Bryant S, Båmstedt U. Growth rate and toxicity of *Prymnesium parvum* and *Prymnesium patelliferum* (haptophyta) in response to changes in salinity, light and temperature. Sarsia. 1998;83:409-18.
8. Manning SR, La Claire JW. Prymnesins: Toxic Metabolites of the Golden Alga, *Prymnesium parvum* Carter (Haptophyta). Mar Drugs. 2010;8:678-704.
9. Wang DZ. Neurotoxins from Marine Dinoflagellates: A Brief Review. Mar Drugs. 2008;6:349-71.
10. Igarashi T, Oshima Y, Murata M, Yasumoto T, editors. Chemical studies on prymnesins isolated from *Prymnesium parvum*. Harmful Marine Algal Blooms: Proceedings of the Sixth International Conference on Toxic Marine Phytoplankton, October 1993, Nantes, France; 1995.
11. Igarashi T, Satake M, Yasumoto T. Prymnesin-2: A Potent Ichthyotoxic and Hemolytic Glycoside Isolated from the Red Tide Alga *Prymnesium parvum*. J Am Chem Soc. 1996;118:479-80.
12. Igarashi T, Satake M, Yasumoto T. Structures and Partial Stereochemical Assignments for Prymnesin-1 and Prymnesin-2: Potent Hemolytic and Ichthyotoxic Glycosides Isolated from the Red Tide Alga *Prymnesium parvum*. J Am Chem Soc. 1999;121:8499-511.
13. Rasmussen SA, Meier S, Andersen NG, Blossom HE, Duus JØ, Nielsen KF, et al. Chemodiversity of Ladder-Frame Prymnesin Polyethers in *Prymnesium parvum*. J Nat Prod. 2016;79:2250-6.
14. Hems ES, Wagstaff BA, Saalbach G, Field RA. CuAAC click chemistry for the enhanced detection of novel alkyne-based natural product toxins. Chem Commun. 2018;54:12234-7.
15. Binzer SB, Svenssen DK, Daugbjerg N, Alves-de-Souza C, Pinto E, Hansen PJ, et al. A-, B- and C-type prymnesins are clade specific compounds and chemotaxonomic markers in *Prymnesium parvum*. Harmful Algae. 2019;81:10-7.
16. Watson S. Literature Review of the Microalga *Prymnesium parvum* and its associated toxicity. Texas Parks and Wildlife Department. 2001.
17. Hagström JA, Sengco MR, Villareal TA. Potential Methods for Managing *Prymnesium parvum* Blooms and Toxicity, With Emphasis on Clay and Barley Straw: A Review. JAWRA Journal of the American Water Resources Association. 2010;46:187-98.
18. Barkoh A, Paret JM, Lyon DD, Begley DC, Smith DG, Schlechte JW. Evaluation of Barley Straw and a Commercial Probiotic for Controlling *Prymnesium parvum* in Fish Production Ponds. N Am J Aquacult. 2008;70:80-91.

19. Rodgers Jr JH, Johnson BM, Bishop WM. Comparison of Three Algaecides for Controlling the Density of *Prymnesium parvum*. JAWRA Journal of the American Water Resources Association. 2010;46:153-60.
20. Holdway PA, Watson RA, Moss B. Aspects of the ecology of *Prymnesium parvum* (Haptophyta) and water chemistry in the Norfolk Broads, England. Freshwat Biol. 1978;8:295-311.
21. Wagstaff BA, Hems ES, Rejzek M, Pratscher J, Brooks E, Kuhaudomlarp S, et al. Insights into toxic *Prymnesium parvum* blooms: the role of sugars and algal viruses. Biochem Soc Trans. 2018;46:413-21.
22. Authority B. Broads Plan 2017. 2017.
23. Wagstaff B, Vladu I, Barclay J, Schroeder D, Malin G, Field R. Isolation and Characterization of a Double Stranded DNA Megavirus Infecting the Toxin-Producing Haptophyte *Prymnesium parvum*. Viruses. 2017;9:40.
24. Bürgmann H, Widmer F, Sigler WV, Zeyer J. mRNA extraction and reverse transcription-PCR protocol for detection of nifH gene expression by *Azotobacter vinelandii* in soil. Appl Environ Microbiol. 2003;69:1928-35.
25. Caporaso JG, Lauber CL, Walters WA, Berg-Lyons D, Huntley J, Fierer N, et al. Ultra-high-throughput microbial community analysis on the Illumina HiSeq and MiSeq platforms. The ISME journal. 2012;6:1621.
26. Caporaso JG, Kuczynski J, Stombaugh J, Bittinger K, Bushman FD, Costello EK, et al. QIIME allows analysis of high-throughput community sequencing data. Nat Methods. 2010;7:335.
27. Galluzzi L, Bertozzini E, Penna A, Perini F, Pigalarga A, Graneli E, et al. Detection and quantification of *Prymnesium parvum* (Haptophyceae) by real-time PCR. Lett Appl Microbiol. 2008;46:261-6.
28. Zamor RM, Glenn KL, Hambright KD. Incorporating molecular tools into routine HAB monitoring programs: Using qPCR to track invasive *Prymnesium*. Harmful Algae. 2012;15(Supplement C):1-7.
29. Ludwig W, Strunk O, Westram R, Richter L, Meier H, Yadhukumar, et al. ARB: a software environment for sequence data. Nucleic Acids Res. 2004;32:1363-71.
30. Guillard RR, Ryther JH. Studies of marine planktonic diatoms: I. *Cyclotella nana* Hustedt, and *Detonula confervacea* (Cleve) Gran. Can J Microbiol. 1962;8:229-39.
31. Andersen RA, Kawachi M. Microalgae isolation techniques. Algal culturing techniques. 2005:83.
32. Porter KG, Feig YS. The use of DAPI for identifying and counting aquatic microflora. Limnol Oceanogr. 1980;25:943-8.
33. Smalley NE, Taipale S, De Marco P, Doronina NV, Kyrpides N, Shapiro N, et al. Functional and genomic diversity of methylotrophic Rhodocyclaceae: description of *Methyloversatilis discipulorum* sp. nov. Int J Syst Evol Microbiol. 2015;65:2227-33.
34. Khan ST, Fukunaga Y, Nakagawa Y, Harayama S. Emended descriptions of the genus *Lewinella* and of *Lewinella cohaerens*, *Lewinella nigricans* and *Lewinella persica*, and description of *Lewinella lutea* sp. nov. and *Lewinella marina* sp. nov. Int J Syst Evol Microbiol. 2007;57:2946-51.
35. Green DH, Echavarri-Bravo V, Brennan D, Hart MC. Bacterial diversity associated with the coccolithophorid algae *Emiliania huxleyi* and *Coccolithus pelagicus* f. braarudii. BioMed research international, 2015. 2015.

36. Manning SR, La Claire Ii JW. Isolation of polyketides from *Prymnesium parvum* (Haptophyta) and their detection by liquid chromatography/mass spectrometry metabolic fingerprint analysis. Anal Biochem. 2013;442:189-95.
37. Baker JW, Grover JP, Brooks BW, Ureña-Boeck F, Roelke DL, Errera R, et al. Growth and toxicity of *Prymnesium parvum* (haptophyta) as a function of salinity, light, and temperature. J Phycol. 2007;43:219-27.
38. Matthijs HC, Visser PM, Reeze B, Meeuse J, Slot PC, Wijn G, et al. Selective suppression of harmful cyanobacteria in an entire lake with hydrogen peroxide. Water Res. 2012;46:1460-72.
39. Burson A, Matthijs HCP, de Bruijne W, Talens R, Hoogenboom R, Gerssen A, et al. Termination of a toxic *Alexandrium* bloom with hydrogen peroxide. Harmful Algae. 2014;31:125-35.
40. Ding Y, Gan N, Li J, Sedmak B, Song L. Hydrogen peroxide induces apoptotic-like cell death in *Microcystis aeruginosa* (Chroococcales, Cyanobacteria) in a dose-dependent manner. Phycologia. 2012;51:567-75.
41. Gobler CJ, Berry DL, Dyhrman ST, Wilhelm SW, Salamov A, Lobanov AV, et al. Niche of harmful alga *Aureococcus anophagefferens* revealed through ecogenomics. Proceedings of the National Academy of Sciences. 2011;108:4352.
42. Driscoll WW, Espinosa NJ, Eldakar OT, Hackett JD. Allelopathy as an emergent, exploitable public good in the bloom-forming microalga *Prymnesium parvum*. Evolution. 2013;67:1582-90.
43. Bertin MJ, Zimba PV, Beauchesne KR, Huncik KM, Moeller PDR. The contribution of fatty acid amides to *Prymnesium parvum* Carter toxicity. Harmful Algae. 2012;20:117-25.
44. Henrikson JC, Gharfeh MS, Easton AC, Easton JD, Glenn KL, Shadfan M, et al. Reassessing the ichthyotoxin profile of cultured *Prymnesium parvum* (golden algae) and comparing it to samples collected from recent freshwater bloom and fish kill events in North America. Toxicon. 2010;55:1396-404.
45. Yorke JA, Anderson WN. Predator-Prey Patterns. Proceedings of the National Academy of Sciences. 1973;70:2069-71.
46. Rach J, Schreier TM, Howe G, Redman S. Effect of species, life stage, and water temperature on the toxicity of hydrogen peroxide to fish. The Progressive Fish-Culturist. 1997;59:41-6.
47. Avendaño-Herrera R, Magariños B, Irgang R, Toranzo AE. Use of hydrogen peroxide against the fish pathogen *Tenacibaculum maritimum* and its effect on infected turbot (*Scophthalmus maximus*). Aquaculture. 2006;257:104-10.

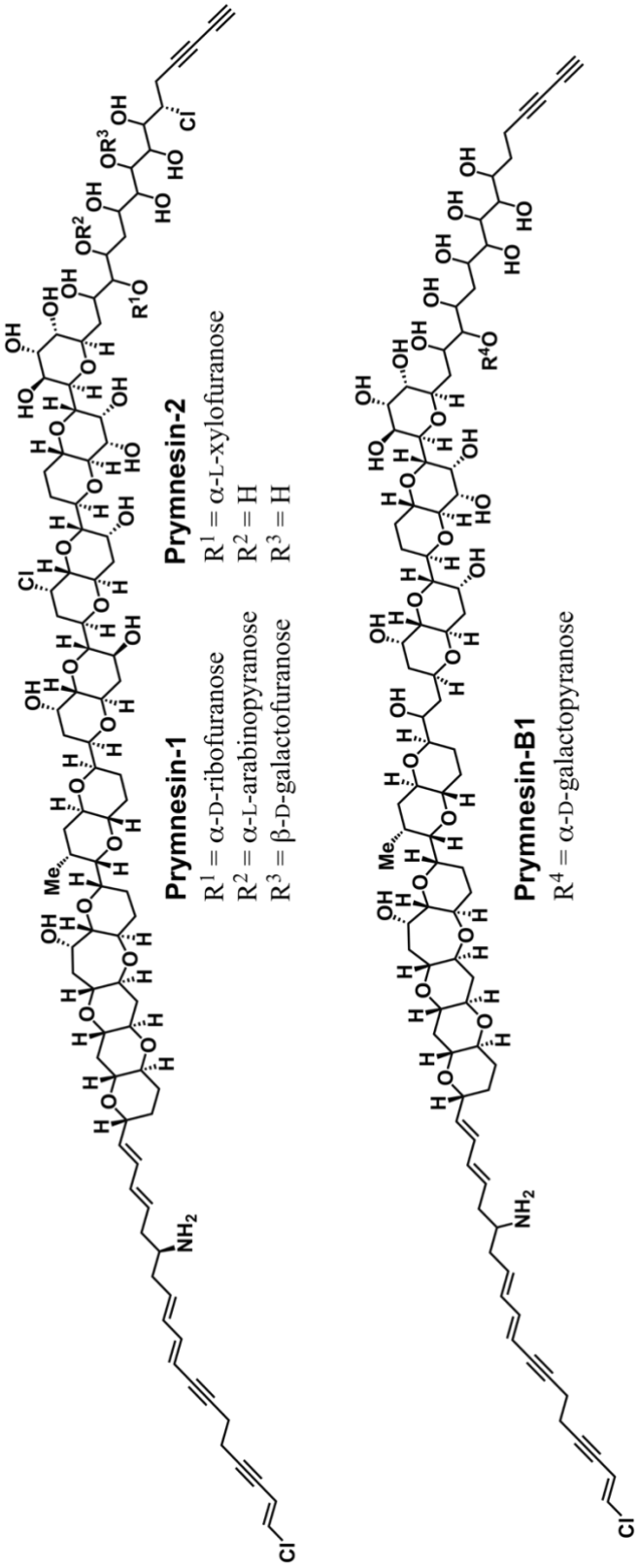

Figure 1 | Chemical structure of prymnesin-1, -2, and -B1. (10, 13). Adapted from Hems *et al.* (14).

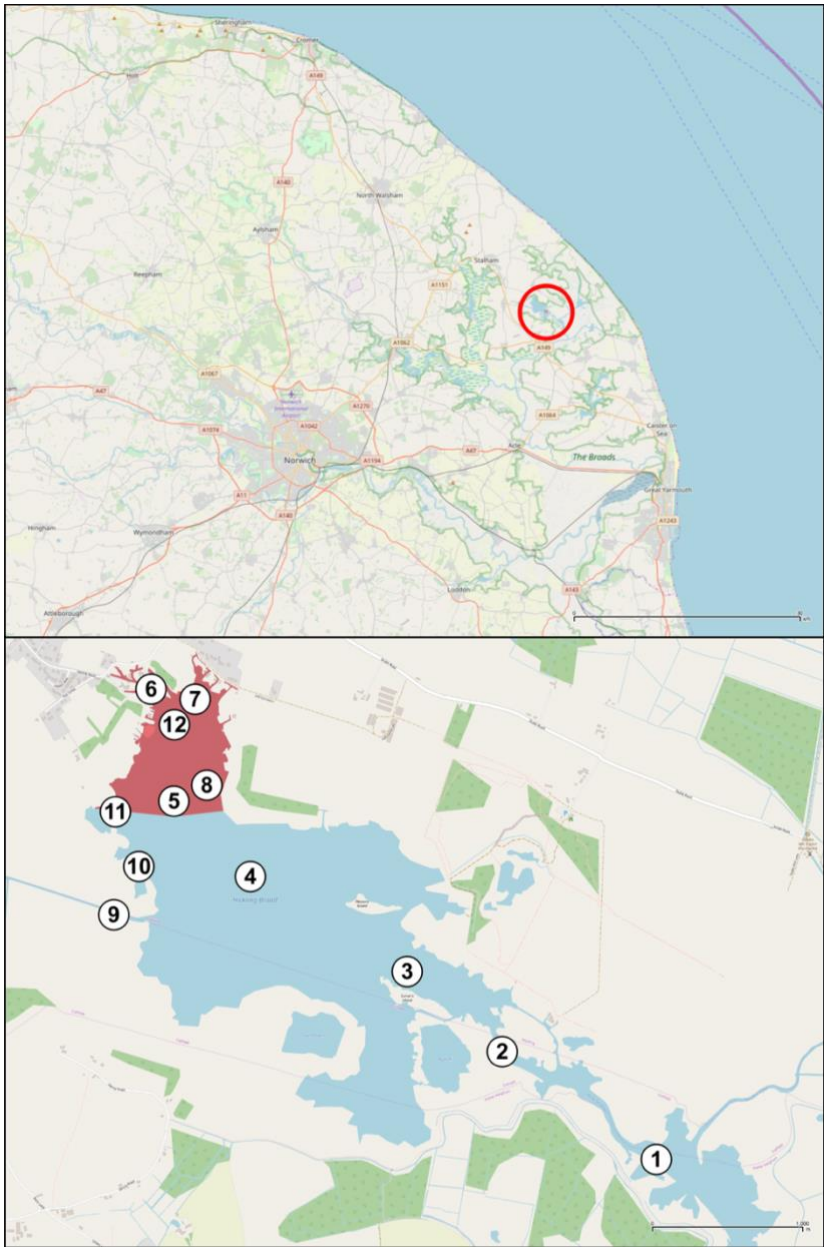

Figure 2 | Map of wider Norfolk, UK, and sampling points on Hickling Broad. Top – Map of Norfolk and the Hickling Broad highlighted by a red circle. Bottom - Map showing the sampling points covering Hickling Broad established during the harmful *P. parvum* bloom in April 2015 and retained throughout the whole sampling campaign. The red shaded area represents the area where the majority of fish kills were observed during the bloom. Sample point 12 was added later as an additional sampling point and is not included in some analyses. Map was generated using QGIS with OSM standard map. Scale bar (top) – 30 km. Scale bar (bottom) – 1 km.

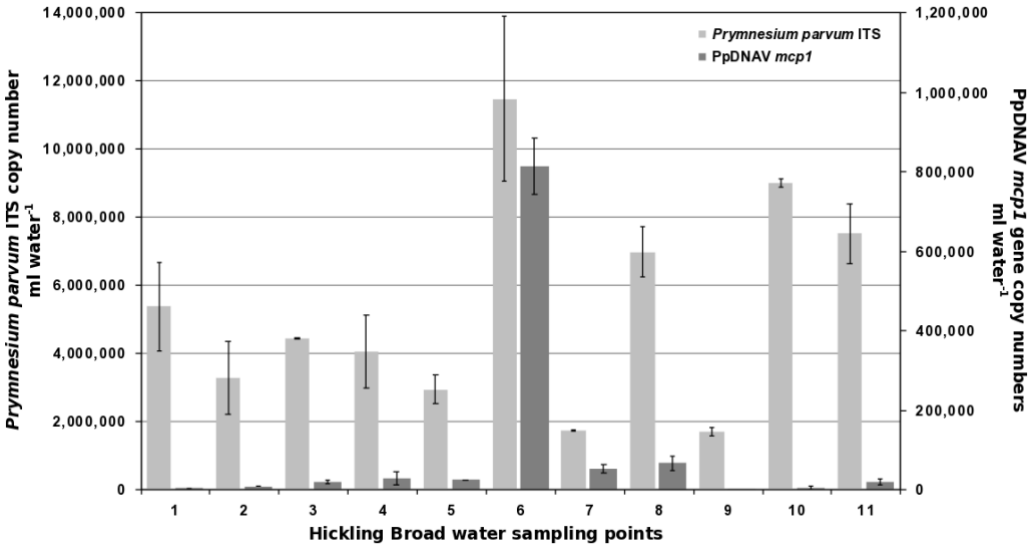

Figure 3 | Abundance of *P. parvum* and PpDNAV in Hickling Broad water samples during the harmful bloom in April 2015. Abundance of *P. parvum specific* ITS genes (light grey bars) and PpDNAV *mcp1* genes (dark grey bars) was measured by qPCR of total DNA extracted from Hickling Broad water samples collected during the harmful *P. parvum* bloom in April 2015. Values represent the average of three replicates with their respective standard deviations. Numbers refer to sampling sites on Hickling Broad (see Fig. 1).

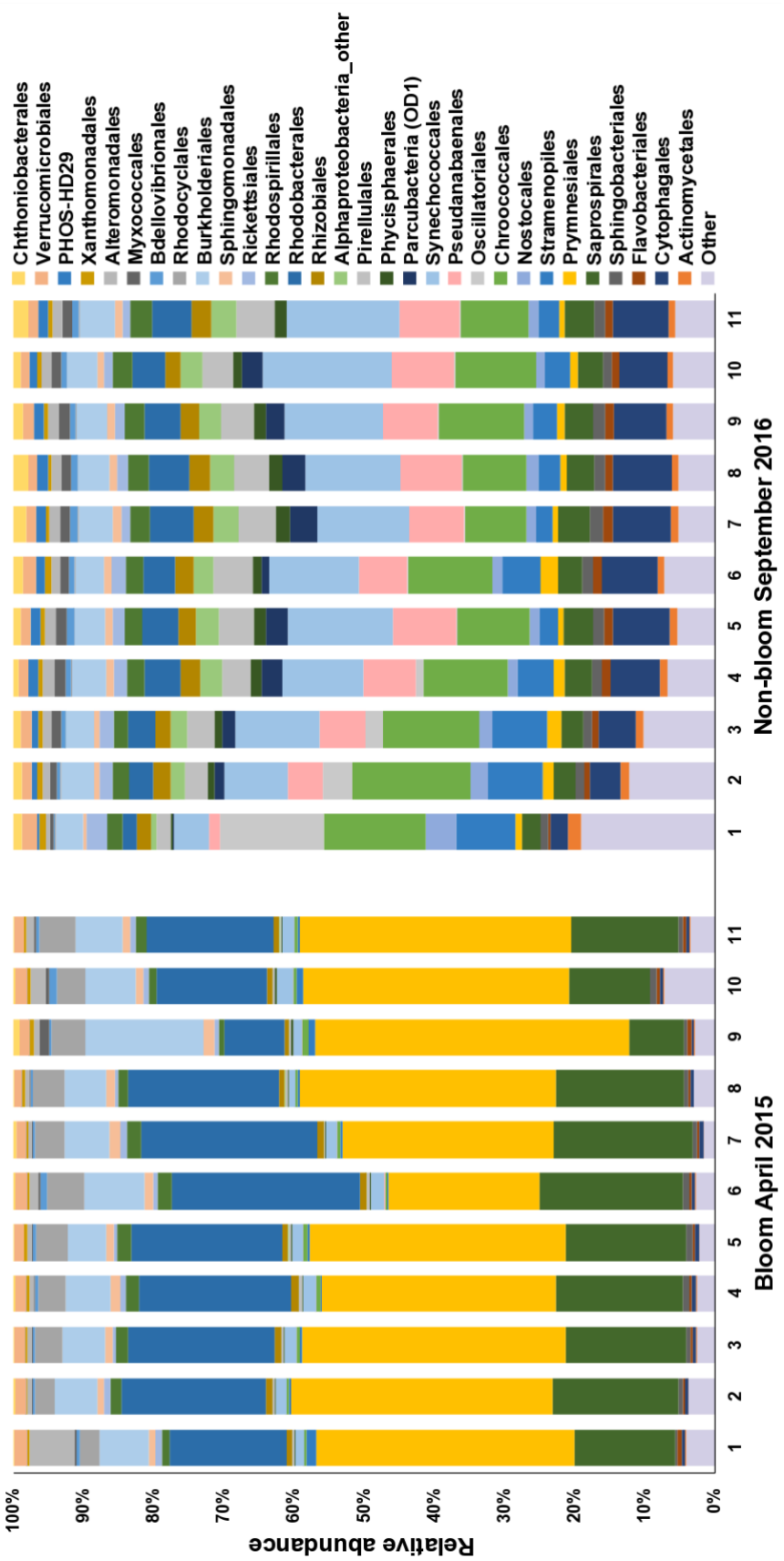

Figure 4 | Microbial community profiles of the harmful *P. parvum* bloom compared to non-bloom water on Hickling Broad, obtained by 16S rRNA gene amplicon sequencing. Profiles

are derived from total DNA extracted from Hickling Broad water samples collected at consistent sampling points during the harmful *P. parvum* bloom in April 2015 and during a non-bloom phase in September 2016. Relative abundance of taxonomic groups within each sample is shown at the order level as percentages. Only taxa with a combined relative abundance of ≥ 0.1% are shown. Numbers refer to sampling sites on Hickling Broad (see Fig. 1).

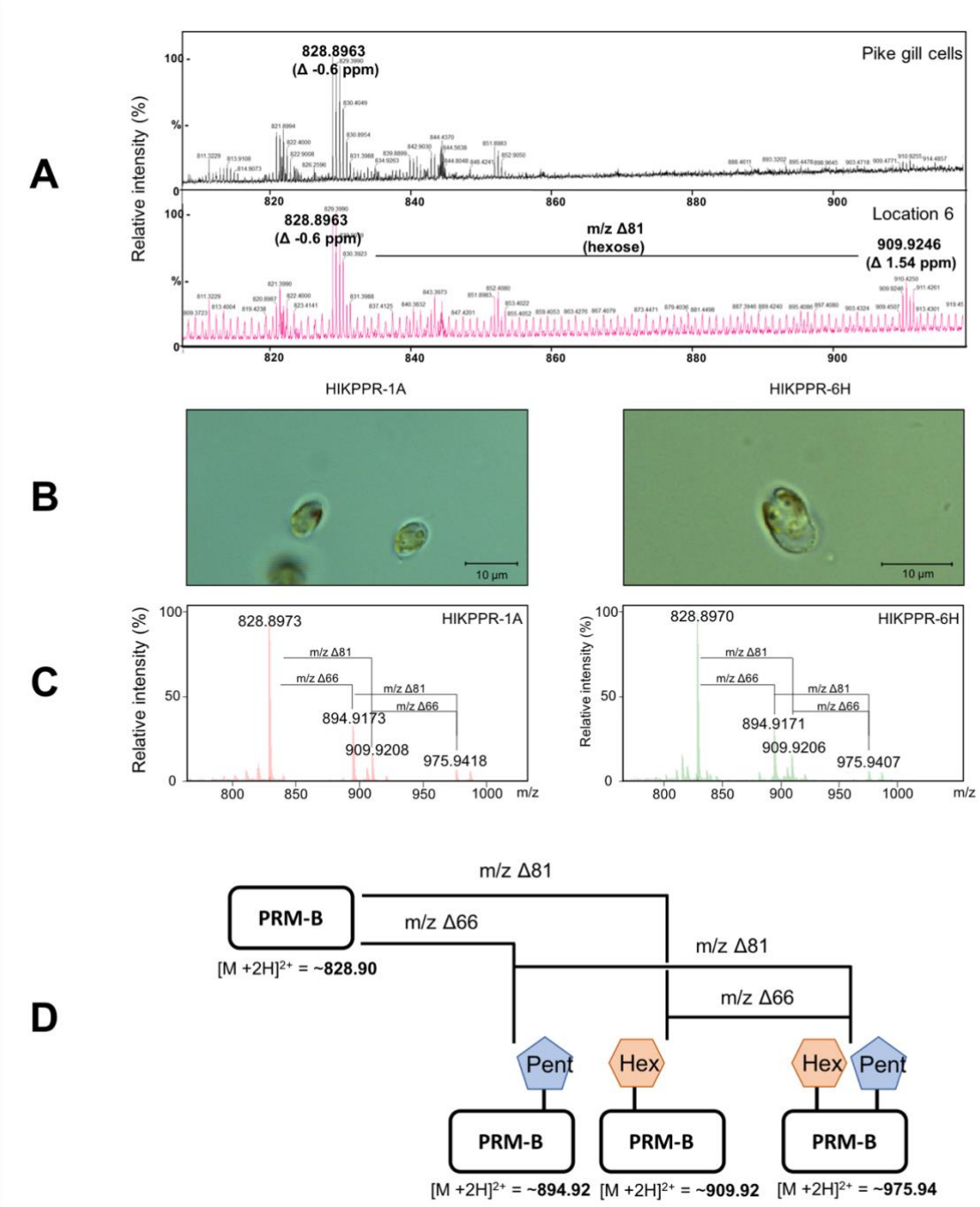

Figure 5 | MS-based identification of B-type prymnesins from environmental samples and isolates of *P. parvum* from Hickling Broad. (**A**) ESI-MS spectrum showing detection of the diagnostic signal (m/z 828.8963, Δ -0.6 ppm) for the backbone of the B-type prymnesins from Pike gill cells (top), and water sample 6 (bottom) taken during a toxic bloom. ESI-MS signal corresponding to the singly glycosylated form of the toxin (m/z 909.9246, Δ 1.54 ppm) could also be seen in the water sample from location 6. (**B**) Light microscopy images of *P. parvum* HIK PR1A (left) and HIK PR6H (right). (**C**) ESI-MS spectra showing detection of the diagnostic signals for the aglycone (m/z ~828.9), mono glycosylated with a pentose (m/z ~894.9), mono glycosylated with a hexose (m/z ~909.9), and double glycosylated with pentose and hexose (m/z ~ 975.9) forms of the B-type prymnesins, from HIK PR1A (left) and HIK PR6H (right). All masses observed for the toxins have errors less than Δ 3 ppm with the exception of m/z 975.9407 of the intact double glycosylated toxin from HIKPPR-6H which has an error of Δ -3.8 ppm. (**D**) Schematic of proposed prymnesin-B fragmentation events observed in ESI-MS spectra (A) and (C). Losses of m/z = 66 or m/z = 81 correspond to the loss of pentose or hexose units from the toxin backbone, respectively.

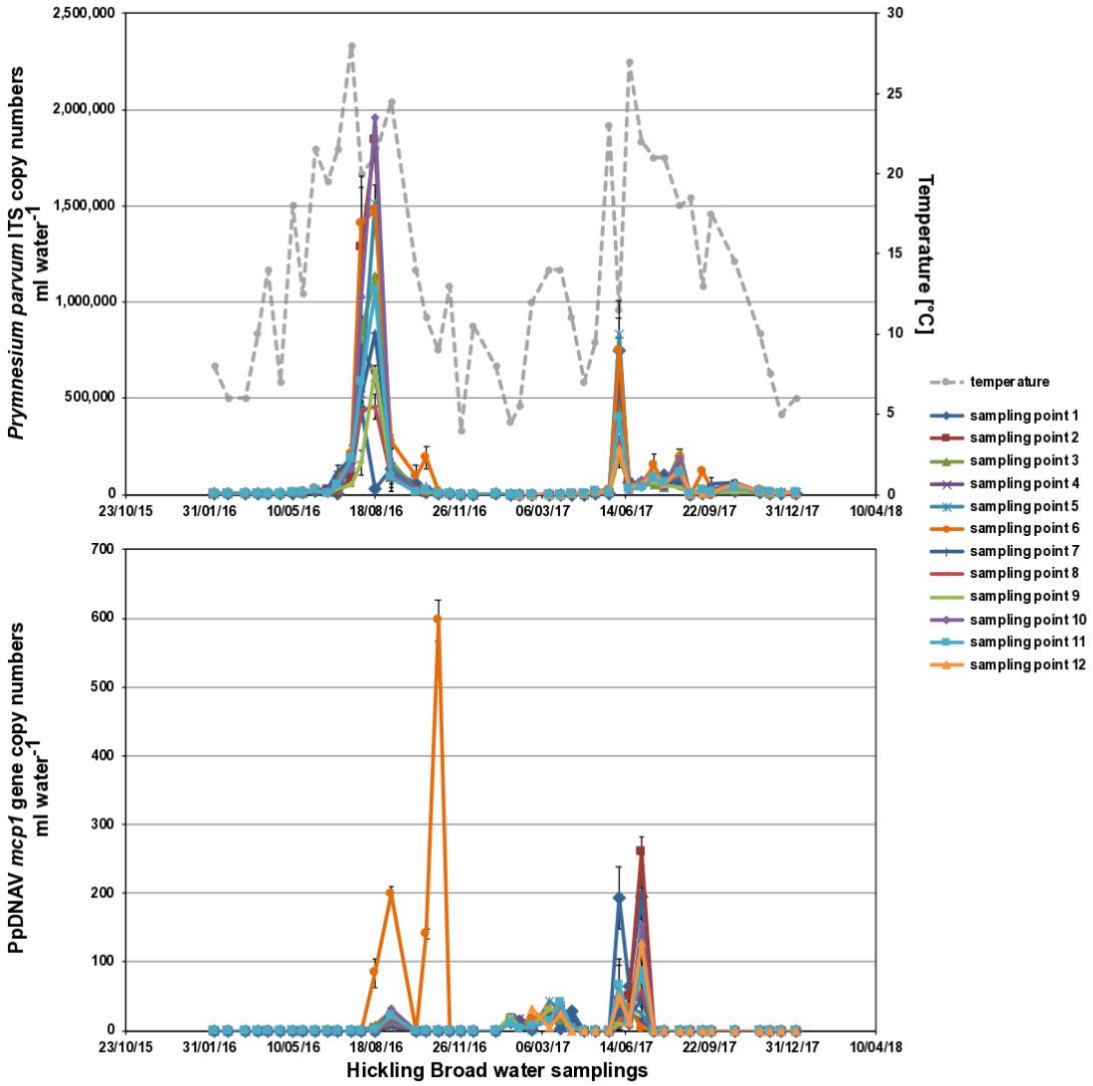

Figure 6| 2-year survey of *P. parvum* and PpDNAV population dynamics on Hickling Broad. Abundance of *P. parvum* specific ITS genes and PpDNAV *mcp1* genes was measured by qPCR of total DNA extracted from Hickling Broad water samples collected at consistent sampling points every 2-4 weeks from January 2016-January 2018 (see Fig. 2). Values represent the average of three replicates with their respective standard deviations.

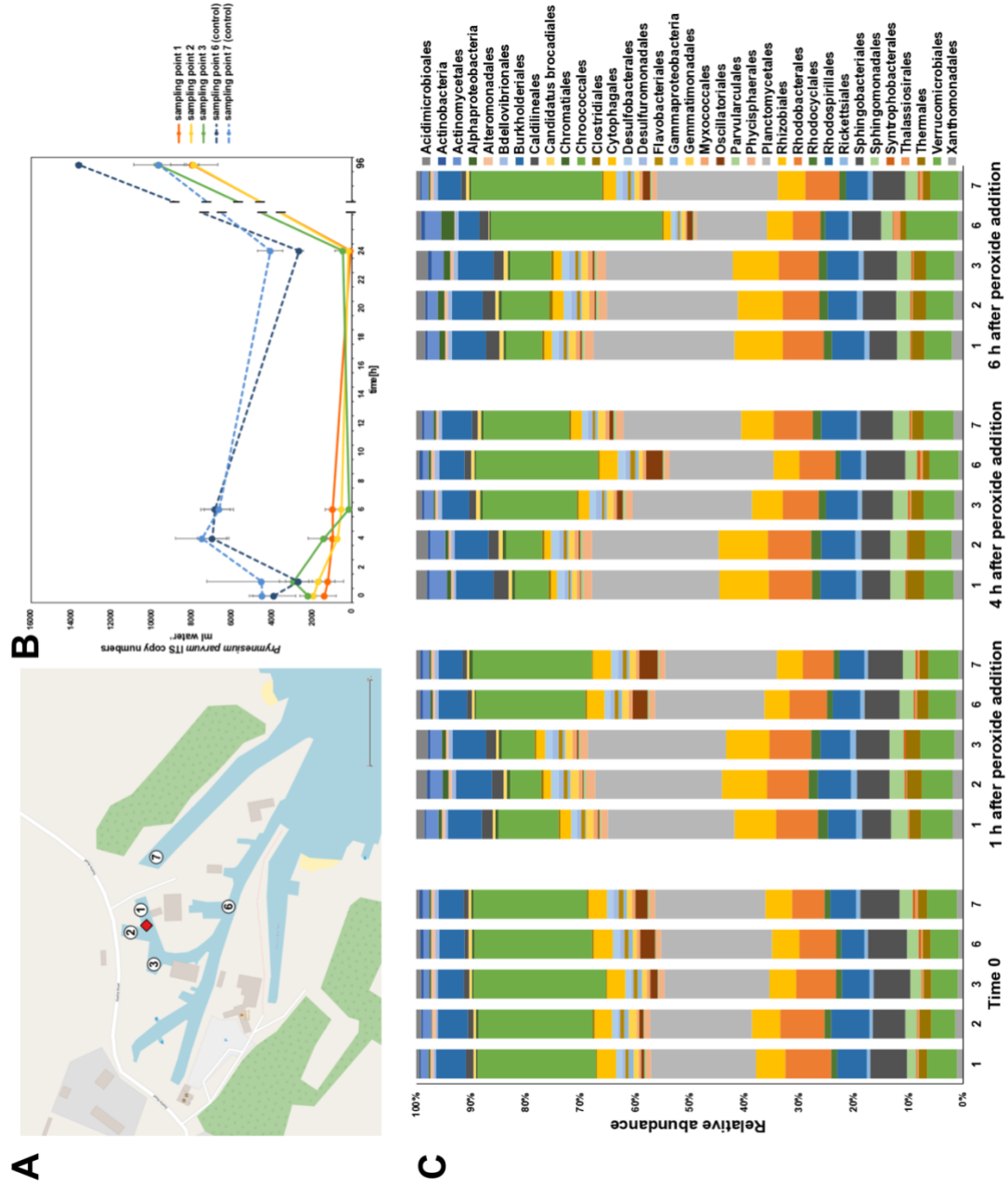

Figure 7 | Effect of peroxide treatment on the abundance of *P. parvum* and microbial community profiles in Hickling Broad water samples. (**A**) Study site on Hickling Broad where

hydrogen peroxide was applied (locations 1-3), and control locations outside of the dyke (locations 6, 7). Scale bar represents 100 m. (**B**) Abundance of *P. parvum specific* ITS gene was measured by qPCR of total DNA extracted from Hickling Broad water samples collected over a time series before (T0) and after *in situ* peroxide treatment (1 h, 4 h, 6 h, 24 h, and 96 h) in June 2017. Values represent the average of three replicates with their respective standard deviations. (**C**) Microbial community profiles derived from total DNA extracted from Hickling Broad water samples collected over a time series before (T0) and after *in situ* peroxide treatment (1 h, 4 h, and 6 h) in June 2017. Relative abundance of taxonomic groups within each sample is shown at the order level as percentages. Only taxa with a combined relative abundance of > 0.1% are shown. Numbers refer to sampling sites during the peroxide trial.